JASA ARTICLE

A necessary condition for double-decay envelopes in stringed instruments

Jim Woodhouse[a)]
Department of Engineering, Cambridge University, Trumpington Street, Cambridge, CB2 1PZ, United Kingdom

ABSTRACT:
Measurements of body vibration characteristics of five different stringed musical instruments have been used to address the question of whether and when they might be expected to produce transient response featuring a "double decay" sound profile. The phenomenon has been well documented and studied in the context of the piano but has not been systematically studied for other instruments. The results show considerable variation among instruments. The piano is indeed predicted to show double decays over most of its range. In the tested guitar, by contrast, double decays are likely to be confined to a few notes near strong body resonances. Other instruments fall between these extremes. The lute and the mandolin, both normally strung with double strings, should both exhibit double decays over much of their playing range, especially towards the higher end. The banjo is single-strung but is also predicted to show strong double decays, especially for higher notes in its range. © *2021 Acoustical Society of America.*
https://doi.org/10.1121/10.0009012
(Received 5 September 2021; revised 20 November 2021; accepted 22 November 2021; published online 16 December 2021)
[Editor: Andrew Morrison] Pages: 4375–4384

I. INTRODUCTION

In a classic paper from the 1970s, Weinreich (1977) analysed the behaviour of a pair of piano strings, coupled at the bridge by the dynamics of the piano soundboard. He used a simple model with two degrees of freedom representing the fundamental modes of the two separate strings to explore the range of possible behaviours when the tuning of the two strings was varied slightly around the condition of perfect unison.

A major conclusion was that the two coupled modes often have significantly different loss factors. This conclusion is particularly obvious for the case where the two strings are tuned in perfect unison. The system then has a plane of symmetry, and the coupled modes must be symmetric or antisymmetric in that plane. The antisymmetric mode has the two strings moving in opposite directions so that the net force exerted on the bridge is zero and no energy is lost to the soundboard. The symmetric mode has the two strings moving together, exerting a large combined force on the bridge. The bridge moves in response to this force, so that the effective length of the string is changed and the frequency is shifted a little, and also some energy is lost to the soundboard so that the loss factor is higher.

It follows that when the note is played, the envelope of the transient response tends to show a characteristic "double-decay" profile. The mode with the faster decay is automatically associated with more soundboard motion and therefore more sound radiation so that it usually dominates the early sound. However, sooner or later, its amplitude will fall below that of the slower-decaying mode, which will then take over and dominate the "after-sound." Weinreich (1977) showed that the detailed envelope is sensitive to the degree of mistuning of the strings. This provides a resource for a skilled piano tuner to adjust the sound profile of the note.

Double decays have indeed been reported experimentally in piano notes (Martin, 1947; Weinreich, 1977), and many authors, Weinreich included, have suggested that the double-decay effect is an important ingredient of the sound. This seems a very plausible claim, but there do not appear to be any published studies using formal psychoacoustical testing to verify this, or to explore such questions as the threshold of perception in terms of the two decay rates and the relative amplitudes of their associated sounds.

The Weinreich (1977) paper is very well known, and some other authors have discussed the problem using models closely related to his; see, for example, section 6.3 of Chaigne and Kergomard (2013). The phenomenon of double decays has also been taken up in various work from the sound synthesis community; see, for example, Lee *et al.* (2010) and Välimäki *et al.* (1996). However, it appears that no-one has subsequently revisited this problem to explore extensions to other stringed instruments. However, the piano is by no means the only instrument involving paired strings arranged in "courses": other examples include the 12-string guitar, the mandolin, and the lute.

In any case, as Weinreich (1977) pointed out, stringed instruments can show the characteristic double-decay envelope profile without using paired strings. The two polarisations of transverse motion in a single string can produce a similar effect. Usually, the soundboard vibrates predominantly in the normal direction. In that case, string motion in the plane perpendicular to the soundboard can couple well

[a)]Electronic mail: jw12@cam.ac.uk, ORCID: 0000-0002-6645-1635.

to soundboard motion, but the polarisation parallel to the soundboard surface will couple less strongly. The mode involving string motion in the perpendicular plane will tend to make more sound, and also decay more rapidly. A double-decay envelope of the resulting radiated sound is likely to be created, and indeed double decays have been reported experimentally in the case of the banjo (Stephey and Moore, 2008). This raises the question of whether double decays are important for the sound of all plucked-string or struck-string instruments, or whether some instruments are more susceptible to the effect than others.

That is the question to be explored in this paper. A very simple criterion will be developed, which gives a necessary condition for a significant double decay to occur (within the assumptions of linear theory). It can be applied equally well to both physical mechanisms. This criterion allows an initial assessment of the likelihood of significant double decays in various stringed instruments, based on a standard measurement of bridge admittance near the attachment point of the string of interest. Examples will be given for a variety of instruments. The analysis of string damping employed in this work shares some features with earlier work on the guitar (Woodhouse, 2004a, 2004b), the lute (Woodhouse, 2017), and the banjo (Woodhouse *et al.*, 2021a, 2021b).

II. WHEN ARE DOUBLE DECAYS IMPORTANT?

A. Damping mechanisms

The physics outlined above will always be present, so in a sense, the double-decay phenomenon must be universal in plucked or struck stringed instruments. However, that does not mean that it is always important for the sound: the double-decay behaviour needs to be sufficiently marked to exceed a threshold of perception. Both physical mechanisms involve two (or more) modes. The player excites some initial mixture of these modes, the details depending on the gesture (for example plucking angle on a guitar string or use of the *una corda* pedal on a piano). The resulting sound will involve a linear combination of the modal responses, and if a clear double decay is to arise an obvious necessary condition is that the loss factors of these modes must be significantly different. If not, the modes will decay at the about same rate and there is no mechanism to differentiate early sound from after-sound, whatever the player may do in the way of varying their gesture.

To assess the conditions under which a significant difference of modal loss factors can arise, the damping mechanisms affecting string vibration need to be considered. This is a subject that has been explored extensively in the past, and experimentally-validated models for the different damping mechanisms are already well established (Valette, 1995; Woodhouse, 2004b; Woodhouse *et al.*, 2021a). There are three main mechanisms, each associated with a separate loss factor. The sum of the three gives the total modal loss factor, which is the inverse of the Q-factor.

The first mechanism is energy loss through the bridge into the body of the instrument. Suppose string j has wave admittance $Y_{0j} = [T_j m_j]^{-1/2}$ where T_j is its tension and m_j its mass per unit length. If the relevant bridge admittance at frequency ω is $Y(\omega)$ then provided the ratio Y/Y_{0j} is small in magnitude the associated loss factor for mode n of the string is given in terms of the real part of the admittance (Woodhouse *et al.*, 2021a) by

$$\eta_b \approx \frac{2\mathrm{Re}(Y)}{\pi n Y_{0j}}. \tag{1}$$

A string also has intrinsic damping, coming mainly from two sources: one is associated with viscosity in the surrounding air, the other with viscoelasticity of the string. The air damping term is given by Fletcher and Rossing (1998) in the form

$$\eta_{air} \approx \frac{\rho_a}{\rho}\frac{2\sqrt{2}M + 1}{M^2}, \tag{2}$$

where ρ is the string's density, ρ_a is the density of air, and

$$M = \frac{d}{4}\sqrt{\frac{2\pi f_n}{\eta_a}}, \tag{3}$$

where d is the string diameter, f_n is the frequency of the nth string mode and η_a is the kinematic viscosity of air. Textbook values can be used: $\rho_a = 1.2$ kg/m^3 and $\eta_a = 1.5 \times 10^{-5}$ m^2/s.

Energy loss from viscoelasticity in the string arises from the influence of bending stiffness. If the Young's modulus of the string has the complex value $E(1 + i\eta_E)$, an argument based on Rayleigh's principle can be used to yield an expression for the associated loss factor of the nth string mode,

$$\eta_{bend} \approx \frac{E\pi^2 d^2 n^2 \eta_E}{64\rho L^4 f_1^2 + E\pi^2 d^2 n^2}, \tag{4}$$

where the string has vibrating length L and fundamental frequency f_1 (Woodhouse, 2017).

This bending term is small for the low modes but it grows with mode number n. The air damping term, by contrast, is highest for the fundamental mode and falls with increasing n. The result is that intrinsic string damping is normally dominated by air damping for low-order modes. The bending term eventually grows and dominates for high modes, especially for strings made of polymers like nylon or natural gut, or over-wound strings where friction between the windings produces a similar effect. Experimental examples of the dependence on n for a variety of strings can be seen in Woodhouse and Lynch-Aird (2019).

The argument for double decays is then as follows. The two modes of interest are either the in-phase and anti-phase modes of a pair of strings, or two polarisations of a single string. In either case, both modes will have the same intrinsic damping, so for a strong contrast in total damping, it is necessary that one of the modes can lose significantly more

https://doi.org/10.1121/10.0009012

energy through the bridge than the other: the difference has to be at least comparable with the intrinsic damping in order to separate the total loss factors.

If a string exhibits a double-decay envelope, the effect is almost certainly dominated by the lower modes because they have the longest decay times. For the simplest version of a criterion for a strong double decay effect, it is natural to consider just the fundamental mode (as Weinreich did). The intrinsic damping will then be dominated by air damping, and the criterion will be simply

$$\eta_b \gg \eta_{air}, \tag{5}$$

at the relevant fundamental frequency f_1. In the absence of experimental evidence from psychoacoustical studies of the perception of a double decay, it is not at present possible to put a numerical value on the requirement "$\gg$" in this criterion, in order to predict whether the effect will be audible to human listeners. It would be straightforward to add this information when it becomes available, and also to extend the criterion to include higher modes of the string and the effect of η_{bend}, but the model would become more complicated and the price would be a loss of transparency. For the purposes of this preliminary investigation the simple form of Eq. (5) will be used for all numerical examples.

The criterion [Eq. (5)] embodies some assumptions, deliberately chosen to make it a maximal estimate of the disparity in modal damping. Real instruments will not satisfy these assumptions exactly, and the consequence is that double decays will be less prominent. This is the sense in which the criterion is a necessary condition only: if Eq. (5) is not satisfied, there cannot be a strong double decay (provided that linear theory gives a good approximation to the behaviour), but if it is satisfied, it might still turn out that the decay profile does not in fact exhibit the effect strongly.

The reason for that claim is simply that the less-damped mode has been assumed to lose no energy at all to the instrument body. However, except in very special cases, both modes will drive the soundboard to an extent, for two reasons. For the case of a pair of strings, if they are not tuned to exact unison then both coupled modes will exert some component of force in the normal direction on the soundboard. In any case, a real instrument bridge will always have non-vanishing admittance in the direction parallel to the soundboard. To characterise this effect, a 2×2 admittance matrix must be measured at the bridge (see, for example, Woodhouse, 2004b). The result is that string motion in any polarisation will cause soundboard motion, radiating sound and causing some energy loss.

B. Admittance measurements

To investigate the consequences of the criterion in Eq. (5) requires information about the strings and the instrument body behaviour. Results will be presented for five different stringed instruments, chosen to show a wide range of bridge admittance behaviour and a mixture of single and multiple stringing: a piano, a steel-string guitar, a lute, a mandolin and a banjo. The piano was a Broadwood baby grand of early 20th-century date. The steel-string guitar was a Fylde "Falstaff," one of a set of six measured as part of an earlier project (Carcagno *et al.*, 2018). The strings were Martin 80/20 Bronze, for which physical properties have been previously measured (Woodhouse *et al.*, 2012). The lute was an amateur-built 8-course Renaissance model, strung with a combination of nylon and fluorocarbon monofilaments with properties described in detail elsewhere (Woodhouse and Lynch-Aird, 2019). The mandolin was a small bowl-backed Neapolitan instrument of brand "Stridente," strung with La Bella 770 L strings: plain steel for the top two courses, wire-wrapped steel for the lower two courses. The banjo was a Deering Eagle II, measured for an earlier project (Woodhouse *et al.*, 2021a). The stringing was described in detail in that reference.

For all five instruments, the point mobility was measured on the bridge close to one of the string attachment positions, in the direction normal to the soundboard. These measurements will be referred to as "bridge admittance." For all instruments other than the piano, the initial measurement point was on the bridge saddle between the notches for the first and second strings or courses. The piano was measured near the attachment point for the note A_4, nominal frequency 440 Hz. This note, and the ones near it, employs three plain steel strings with diameter close to 1 mm.

All admittance measurements used a miniature impact hammer (PCB 086D80) to tap on the bridge in the direction normal to the soundboard. Vibration response was measured as near as possible to the excitation point, either with a small accelerometer (Endevco 2222C) or a laser-Doppler vibrometer (Polytec OFV-056). Multiple impulses were recorded at a sampling rate of 40 kHz, using a PC running acquisition and analysis software written in MATLAB. The averaged transfer function and the associated coherence function were calculated. Good coherence was obtained up to approximately 8 kHz in all cases. In the case of accelerometer measurements, the results were integrated to give admittance. The criterion in Eq. (5) relies on the real part of the admittance from Eq. (1), so considerable care was taken over the accuracy of the measured phase: the laser vibrometer, in particular, is prone to phase distortion due to a processing delay.

Measured admittance magnitudes for all five instruments are shown in Fig. 1. The plot is rather crowded, but it is useful to see all the results on the same scale for the purposes of direct comparison. Instruments strung with double strings (mandolin and lute) or triple strings (piano) are shown with solid lines. The guitar and the banjo, normally single-strung, are shown with dashed lines. For reference, the lowest tuned notes of the four portable instruments are as follows: guitar E_2 (82.4 Hz); lute D_2 (73.4 Hz); banjo D_3 (146.8 Hz); mandolin G_3 (196.0 Hz). The measured admittances cover a strikingly wide range of amplitudes; peak levels for the banjo rise some 60 dB above the typical level for the piano.

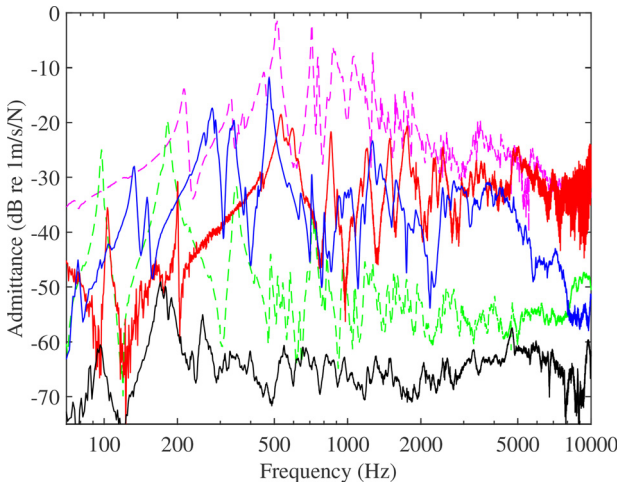

FIG. 1. (Color online) Bridge admittance of five different stringed instruments. Instruments normally strung with multiple strings are shown as solid lines, instruments that are normally single-strung are shown as dashed lines. Black, lowest curve: piano; green dashed, second from the bottom: steel-string guitar; blue: lute; red: mandolin; magenta dashed, highest curve: banjo.

C. Comparison of stringed instruments

Making use of measured admittances like these, the criterion in Eq. (5) can be assessed graphically for any particular combination of instrument and strings by plotting η_b and η_{air} on the same axes, as a function of frequency. Examples for the steel-string guitar and the piano are shown in Fig. 2, making use of the corresponding bridge admittances plotted in Fig. 1. In both plots, the downward-sloping smooth line shows η_{air} while the more spiky curves show alternative versions of η_b, to be explained shortly.

Figure 2(a) is based on the second string of the guitar. The dashed curve shows η_b for the regular guitar with a single string, while the solid curve shows the effect of doubling this string up to simulate the effect of stringing the same guitar body as a 12-string instrument. The curve is simply raised by 6 dB because the combined admittance of the pair of strings is halved (or the impedance is doubled). Where the dashed curve rises significantly above the curve for η_{air}, that indicates that the two polarisations of vibration of a single string could have significantly different damping, and thus create a double decay. Where the solid curve rises above the same curve for η_{air}, that means that the in-phase mode of a pair of strings could have significantly higher damping than the anti-phase mode, and thus create a double decay by that mechanism.

The figure reveals that, in both curves, η_b rises significantly above η_{air} around strong resonance peaks, but in between, it falls much lower. This guitar would be likely to show double decays by the polarisation mechanism on some notes but cannot possibly do so on others, on this particular single string. Doubling up the string as in a 12-string guitar would increase the likelihood of a given note showing a clear double decay because the solid curve is 6 dB above the dashed curve, but the effect will still be patchy. The question of the interaction of string modes with an isolated body resonance will be further discussed in Sec. III.

Figure 2(b) shows that the situation is quite different for the piano. The admittance curve is less peaky: the larger soundboard of the piano exhibits higher modal density and therefore higher modal overlap factor (the ratio of half-power bandwidth to mean modal spacing). The solid curve shows the effect with a triple string, as in the real piano, while the dashed curve shows how things would change if the triple were replaced with a single string. With the triple string, η_b rises above η_{air} by some 20 dB over the entire frequency range above about 160 Hz, so that a marked double decay can be expected for all notes in that range. It is probably no coincidence that on this particular piano, the lowest note using triple sets of plain steel strings is E $\flat_3$, 155.6 Hz. Lower notes use wrapped strings, single or paired, with different string properties: they are not covered by the plot shown here.

For an instrument like the guitar, though, Fig. 2(a) is not the most helpful way to illustrate the potential for double-decay behaviour over the full range of the instrument. It only shows results for one string out of the six, and

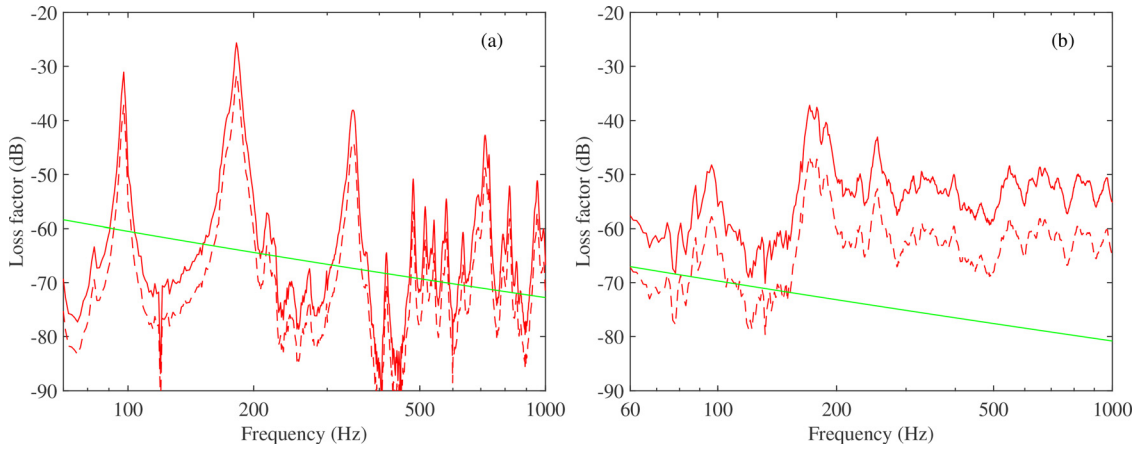

FIG. 2. (Color online) Loss factors η_{air} (green smooth curves) and η_b (red irregular curves) for (a) a steel-string guitar and (b) a piano. In (a), based on the second string, the dashed curve shows the result for a single string and the solid curve shows results for a pair of strings. In (b), based on the note A_4, the solid curve shows results for a triple string as in the real piano, while the dashed curve shows results for a single string with the same properties.

https://doi.org/10.1121/10.0009012

it takes no account of the actual range of fundamental frequencies likely to be played on that string. Figure 3 shows an approximate way to take these objections into account.

A separate line is plotted for each string, over a frequency range from the tuning of the open string up to the note with three times the frequency, corresponding to a musical interval of a 12th, or the 19th fret on the guitar. The plotted quantity is now the difference $\eta_b - \eta_{air}$, still plotted on a dB scale. For a strong double decay to be possible, the curve must rise well above 0 dB, indicated by the dashed line. The conclusion is that this guitar is likely to exhibit clear double decays around the three strong resonances at frequencies near 98, 182, and 348 Hz, but in between the effect will be more marginal. There is a strong gradient across the strings: the low strings produce significantly higher values, while the top string is hardly capable of producing double decays on any note. The plot here is for the regular guitar: if the same guitar body were used to make a 12-string guitar using pairs of strings with the same properties, all the curves would be raised by 6 dB.

The curves in Fig. 3 were all produced using the same bridge admittance, so they are not strictly correct for strings other than the top two. By measuring the admittance separately at each string notch, a more accurate version could be created: an example will be shown in Fig. 6, for the banjo. However, as that figure will illustrate, the difference is not very great. At low frequency where the modal overlap is low, the modal amplitudes will vary across the width of the bridge depending on the proximity of nodal lines, but the general level and trend at higher frequencies will be similar at all positions because the same Skudrzyk mean level would be expected for them all (Skudrzyk, 1980). Because of the "necessary condition" status of the plot, the detailed predictions for individual played notes are likely to be more seriously affected by the other missing factors described at the end of Sec. II A.

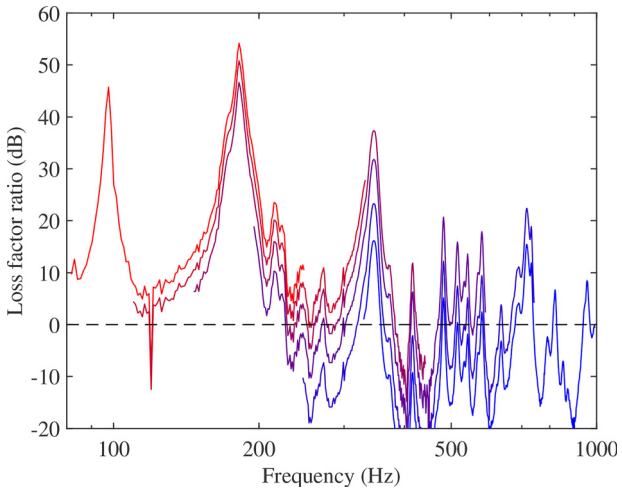

FIG. 3. (Color online) Difference of loss factors $\eta_b - \eta_{air}$ for a steel-string guitar. A separate curve is plotted for each string, over a frequency range from the fundamental of the open string to the frequency at the 19th fret. The colors of curves change from red (lowest string) to blue (highest string).

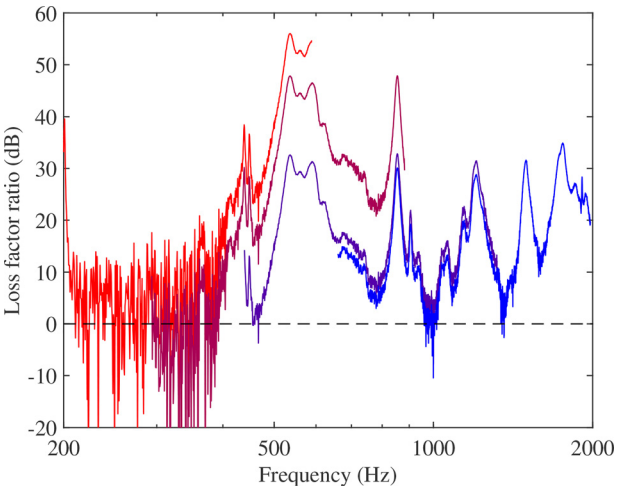

FIG. 4. (Color online) Difference of loss factors $\eta_b - \eta_{air}$ for a mandolin. A separate curve is plotted for each two-string course, over a frequency range from the fundamental of the open string to the frequency at the 19th fret. The colors of curves change from red (lowest course) to blue (highest course).

Figure 4 shows a corresponding plot for the mandolin, an instrument always strung with two-string courses. The pattern contrasts strongly with the guitar. For the lowest octave of the instrument, the curves are so low that no double-decay envelopes would be predicted, but above about 500 Hz most notes on all four courses are candidates for showing double decays.

Figure 5 shows a corresponding plot for the lute. Below about 250 Hz the pattern is somewhat similar to the guitar: high values around two strong resonances, but low values otherwise. However, above 250 Hz, over most of the rest of the playing range of the instrument, values are generally high. This suggests that double decays might be common over much of the playing range, although less so for the top course. Note that the top course is a single string, while the

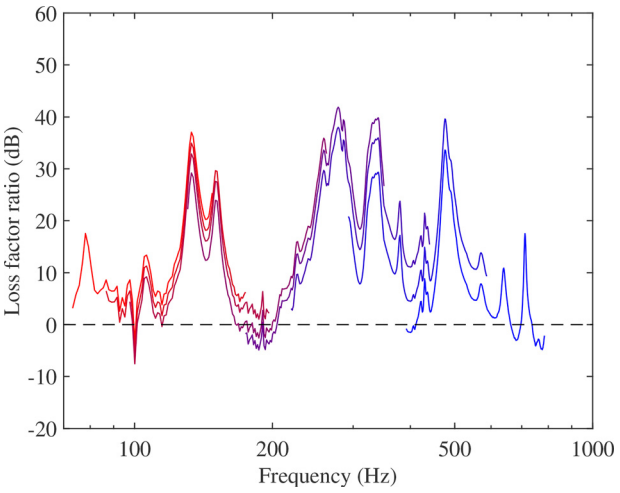

FIG. 5. (Color online) Difference of loss factors $\eta_b - \eta_{air}$ for a lute. A separate curve is plotted for each string or course, over a frequency range from the fundamental of the open string to the frequency at the 12th fret. Note that the top string is single, while all the others are in two-string courses. Colors of curves change from red (lowest) to blue (highest).

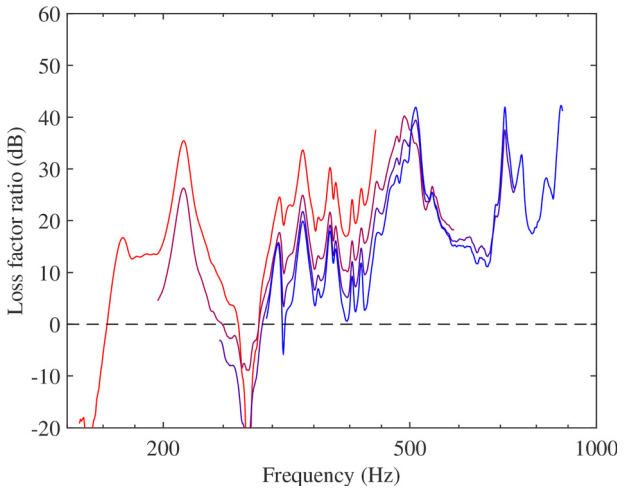

FIG. 6. (Color online) Difference of loss factors $\eta_b - \eta_{air}$ for a banjo. A separate curve is plotted for each string, over a frequency range from the fundamental of the open string to the frequency at the 19th fret. Colors of curves change from red (4th string) to blue (highest string). The 5th string of the banjo has similar properties to the top string, and is not included in the plot.

others are all pairs. The explanation for this traditional stringing pattern is not clear: perhaps it arose originally as a pragmatic response to the expense and fragility of thin gut strings suitable for that course? Figures 8 and 9 of Woodhouse and Lynch-Aird (2019) show that this string is tuned perilously near the breaking stress of gut.

As a final example, Fig. 6 shows a corresponding plot for strings 1–4 of the banjo. The 5th string of the banjo, with a different string length, has similar properties to the top string and is not included. This time a different bridge admittance has been used for each string, so that the curves are not quite parallel copies of the same pattern, but the differences are not great. The curves show a generally rising trend with increasing frequency, and all played notes above about 330 Hz seem likely to produce strong double decays (based on the two string polarisations). The rising trend, not seen in the guitar, mandolin, or lute, is a direct result of the use of a membrane rather than a wooden plate for the "soundboard" of the banjo: it results from the different modal density properties of a membrane and a plate (Woodhouse *et al.*, 2021b).

III. EXTENDING WEINREICH'S MODEL

A. Modelling double strings and a body mode

The bridge admittances shown in Fig. 1 highlight another issue, for which it is of interest to revisit Weinreich's style of modelling based on a modal description. He was able to keep his theoretical model down to only two degrees of freedom by representing the soundboard admittance with a single complex constant. This had the great advantage of allowing closed-form predictions, but the treatment is a little uncomfortable because it mixes time-domain and frequency-domain concepts. This can sometimes lead to apparent paradoxes, such as the well-known causality violation of "ideal hysteretic damping" (e.g., Crandall, 1970).

However, Weinreich's interest was specifically in the piano, and for that case, there is a possible justification for the approach. The piano has a very large soundboard so that in the mid-range of the instrument the fundamentals of all notes fall in a frequency range where the modal overlap factor of the soundboard is not small: Fig. 1 shows this effect clearly. In that case, the magnitude and phase of the bridge admittance will vary relatively slowly, and a natural model would involve using a high-frequency approximation familiar from Statistical Energy Analysis (see, e.g., Lyon and DeJong, 1995). As the modal overlap factor increases, the soundboard admittance tends towards the result for an infinite plate, for which the behaviour is that of a mechanical resistance or dashpot (see, e.g., Cremer *et al.*, 2005). The admittance is then a constant real number, and Weinreich's approach is entirely appropriate.

However, the other stringed instruments studied here are designed to be portable, and have much smaller soundboards. The fundamentals of all low-range played notes fall in a region of low modal overlap for the soundboard, as can be seen in Fig. 1. Of course, the same would be true of the piano in its lowest register, but the relevant frequencies are far below the range shown in Fig. 1.

In the low modal overlap regime, the amplitude and phase of the soundboard admittance will vary rapidly, even over the relatively small frequency range covered by the string resonances and their half-power bandwidths. It is then possible that analysis based on constant admittance will give misleading results. A natural physical approximation to explore this question is to model the body by a single resonance, representing the mode closest in frequency to the fundamental of the note in question. The frequency of this single resonance can be varied relative to the string's frequency, to explore the range of possible coupled behaviour.

Such a model is easy to formulate. Consider two strings of length L, with tension T_j, mass per unit length m_j, and Q-factor Q_j, where $j = 1, 2$. At position $x = 0$ both strings are rigidly anchored, while at $x = L$ they are both attached to a mass m, which is itself attached to a fixed base through a parallel combination of a spring of stiffness k and a dashpot of strength c. The model will only include the first resonance of each string, considered in isolation, so suppose that the displacement of string j is given approximately by

$$w_j(x,t) = b_j(t)\sin\frac{\pi x}{L} + a(t)\frac{x}{L}, \tag{6}$$

where $a(t)$ is the displacement of the oscillator representing the body mode.

The procedure follows the classical method of linear vibration theory (see, e.g., Rayleigh, 1945): first calculate the potential and kinetic energies of the system, then deduce the mass and stiffness matrices for the three degree-of-freedom system parameterised by the vector of generalised coordinates $\mathbf{q} = [a \quad b_1 \quad b_2]^t$. The derivation is closely related to one presented in Woodhouse (2004a), so the

https://doi.org/10.1121/10.0009012

details need not be repeated here. The result for the stiffness matrix is

$$K = \begin{bmatrix} k & 0 & 0 \\ 0 & \frac{\pi^2 T_1}{2L} & 0 \\ 0 & 0 & \frac{\pi^2 T_2}{2L} \end{bmatrix}, \tag{7}$$

and the corresponding mass matrix is

$$M = \begin{bmatrix} m + L(m_1 + m_2)/3 & m_1 L/\pi & m_2 L/\pi \\ m_1 L/\pi & m_1 L/2 & 0 \\ m_2 L/\pi & 0 & m_2 L/2 \end{bmatrix}. \tag{8}$$

Finally, the damping matrix C is needed. The rate of energy dissipation in the body dashpot is $c\dot{a}^2$, so

$$C = \begin{bmatrix} c & 0 & 0 \\ 0 & c_1 & 0 \\ 0 & 0 & c_2 \end{bmatrix}, \tag{9}$$

where the equivalent dashpot strengths of the two string modes are given by

$$c_j = \frac{\pi\sqrt{T_j m_j}}{2Q_j}, \quad j = 1, 2. \tag{10}$$

Note that Q_j here characterises the intrinsic damping of each string mode: the additional damping arising from coupling to the body mode will be found by solving the model.

This model can be readily solved numerically using the first-order approach. The first-order matrix will be 6×6: its eigenvalues and eigenvectors give the complex natural frequencies and mode shapes. There are standard results allowing these to be used to calculate frequency responses or step/impulse responses; see, for example, Newland (1989). For a specific application to coupled string-body vibration in a guitar, see Woodhouse (2004a).

B. Numerical case study

Typical behaviour can be illustrated by a case study, based approximately on the second course of a 12-string guitar. Consider a pair of steel strings with diameter 0.45 mm and length 650 mm, identical except for having slightly different tensions. They are both tuned to frequencies near the nominal B_3 (246.9 Hz), but the two strings are mistuned by a small amount which can be characterised in cents (hundredths of an equal-tempered semitone). Each string resonance, in isolation, is given a Q-factor of 3000.

The single body mode is chosen to match, approximately, one of the strong low-frequency modes of a guitar body, like the ones visible near 100 and 200 Hz in the guitar admittance in Fig. 1. The mode is assigned an effective mass of 0.2 kg and a Q-factor of 40. The stiffness is adjusted to place the resonance frequency at a desired value. Figure 7 shows the "bridge admittance" of this single-mode guitar body, for two cases: one with the resonance frequency close to the played note (dashed line), the other with it a little lower in frequency (solid line).

For both cases, the degree of mistuning between the two strings has been varied through a range of ±8 cents. The system has three degrees of freedom, so it has three modes. (The 6×6 first-order matrix gives six eigenvectors and eigenvalues, but each mode normally appears twice, in complex conjugate form.) The modes all involve motion of the strings and the body resonance, but the modes can generally be divided into two "string modes" and one "body mode" based on how the energy is partitioned between the degrees of freedom. The frequencies and Q-factors have been computed at each stage, and the results for the two "string modes" are plotted in Fig. 8. The red and blue solid lines lines correspond to the admittance plotted with a solid line in Fig. 7; the red and blue dashed lines correspond to the admittance plotted with a dashed line. Red curves indicate the mode in which the two strings vibrate in phase, blue curves indicate the anti-phase mode.

Figure 8(a) shows familiar behaviour usually called "veering" (see, for example, Perkins and Mote, 1986). The pattern is most obvious in the solid curves. The minimum frequency separation occurs when the strings are tuned with exactly the same tension, corresponding to the symmetrical case mentioned earlier. Both cases show qualitatively similar behaviour, but the closest approach of the two curves differs. In the dashed curves, for the case where the body resonance falls very close to the string tuning, the two curves stay well apart throughout the range of mistuning.

Figure 8(b) shows the corresponding modal damping behaviour. The Q-factors vary sensitively with mistuning, especially in the range where the frequencies were actively veering in Fig. 8(a). The two Q-factors reach their maximum and minimum values where the string mistuning ratio is

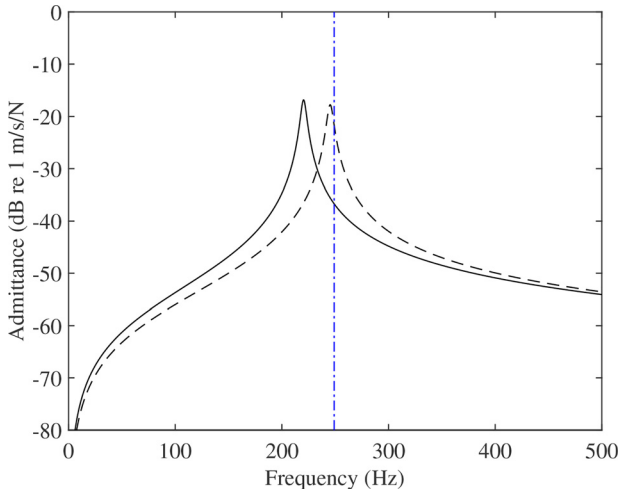

FIG. 7. (Color online) Two examples of bridge admittance of the one-mode body model used in the case study of coupled strings. The vertical line marks the string tuning frequency.

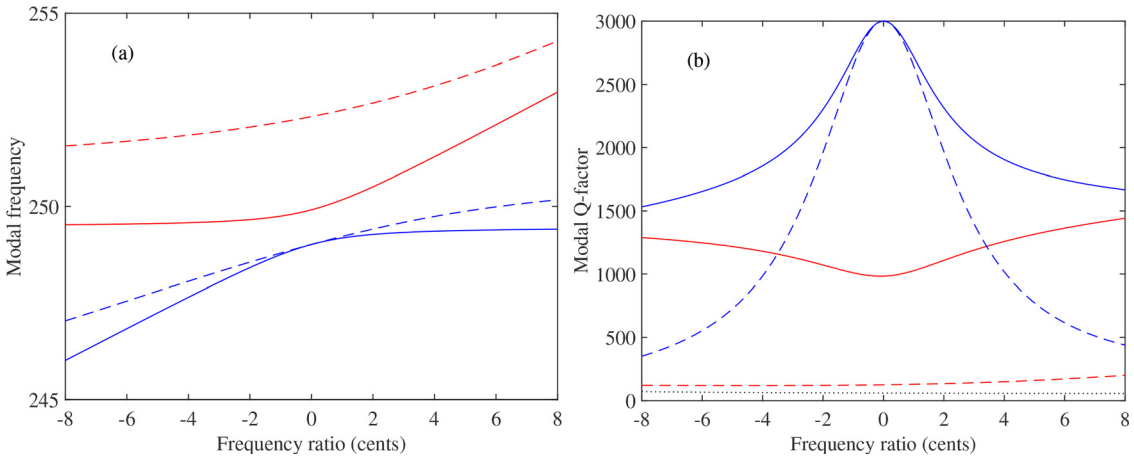

FIG. 8. (Color online) (a) Modal frequency and (b) modal Q-factor as a function of string mistuning frequency ratio. Solid curves show results calculated using the admittance shown as a solid curve in Fig. 7; dashed curves show results for the admittance plotted with a dashed curve. Curves in red indicate modes with the two strings vibrating in the same phase; blue curves show the anti-phase mode.

zero. The maximum Q-value is always 3000 because this is the case of an exactly antisymmetric mode, transferring no energy to the "body." The minimum value varies significantly between the two cases, with the most extreme behaviour in the case where the body resonance falls close to the string tuning. In this case, the Q-factor of a "string mode" comes close to the Q-factor of the "body mode," indicated by the dotted line: coupling is so strong here that the string/body mode distinction is less clear-cut.

Veering behaviour like this was one of the cases mentioned by Weinreich (1977), but he also described others. As discussed above, a relevant case arises if the "body" behaviour at high modal overlap is approximated by the infinite-plate response. This case can be represented in the same numerical model, by making both m and k vanishingly small, then using for the dashpot constant c a value appropriate to the high-frequency behaviour of a guitar soundboard. It can be seen in Fig. 1 that the guitar admittance tends to a value around –50 dB at higher frequency, so the required value is $c \approx 300$ Ns/m.

Using this value of c together with $m = 10^{-3}$ kg and $k = 10^{-3}$ N/m leads to the results shown in Fig. 9, in a similar format to Fig. 8. This time, instead of veering the system exhibits "anti-veering." The two frequencies attract rather than repelling each other, and for a short interval of the mistuning frequency ratio, they merge. In the same range, the two Q-factors diverge from each other, but outside that range they are very similar. This is indeed one of the possible cases described by Weinreich, but it appears that anti-veering behaviour like this does not occur with physically realistic parameter values in the regime of low modal overlap.

Both Figs. 8(b) and 9(b) show that a significant disparity between the two Q-factors can arise under some circumstances and that this disparity can be very sensitive to the degree of mistuning. As explained earlier, such a disparity is a necessary condition to give rise to the double-decay effect. The significance of the veering and anti-veering cases is that with veering, there will always be beats accompanying the decay pattern, whereas with anti-veering there will be no beats.

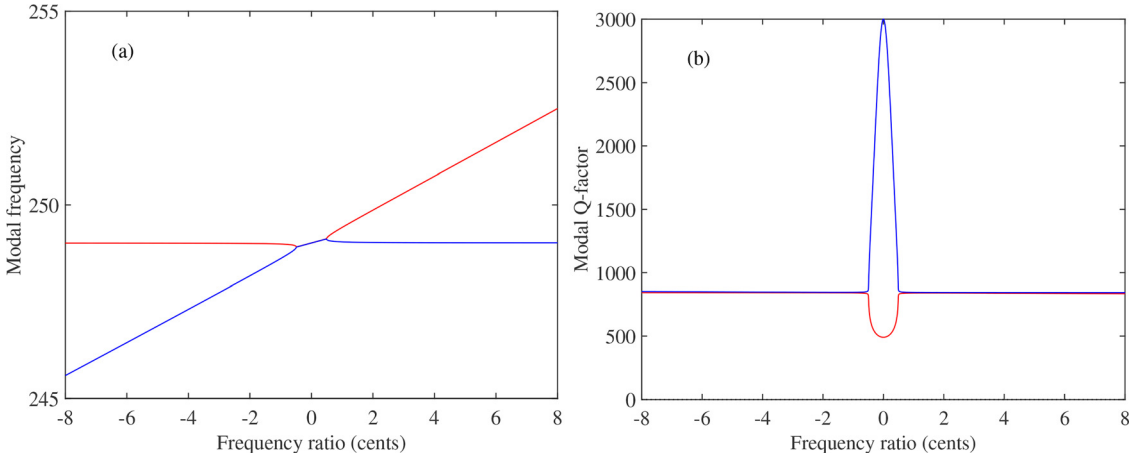

FIG. 9. (Color online) (a) Modal frequency and (b) modal Q-factor as a function of string mistuning frequency ratio, in the same format as Fig. 8, for the case where the bridge admittance is modelled as a dashpot of strength $c = 300$ Ns/m.

https://doi.org/10.1121/10.0009012

More extensive material from this numerical model, including pluck responses, decay envelope plots and synthesised sound examples, is available on an accompanying web site (Woodhouse, 2021).

IV. CONCLUSIONS

Building on a classic study by Weinreich (1977), two different physical mechanisms have been discussed whereby a struck-string or plucked-string musical instrument can exhibit a sound envelope with a double decay. One mechanism involves different behaviour in the two polarisations of motion of a single string, while the other involves coupled motion of two (or more) strings. In the case of multiple strings, the player or piano tuner can exert some control over the form of the envelope by subtle differences in tuning between the strings, although they are nominally tuned to the same note. However, the mechanism involving the two polarisations of a single string has no equivalent of this adjustable mistuning. The only way the player can change the envelope shape is through details of excitation, such as the plucking angle on a plucked-string instrument: but this can only change the relative magnitudes of the two modes, not their respective damping rates.

Weinreich's original study was focussed on the piano, but there are many other stringed instruments, some of them employing pairs of strings in "courses." Results have been shown for five different stringed instruments. The piano stands out from the others (guitar, lute, mandolin, and banjo) because it is the only one for which the fundamental frequencies of most played notes fall in a region where the soundboard exhibits significant modal overlap. The other instruments all show low modal overlap over most or all of the normal playing range. This influences the behaviour of coupled strings, for the instruments featuring paired courses. Based on numerical studies, it seems likely that when modal overlap is low, coupled strings always show "veering" behaviour. The result is that the decay envelope will always be accompanied by beats. When overlap is high, by contrast, the behaviour can switch to a different pattern, illustrated here in the contrast between Figs. 8 and 9. It is then possible to have a double-decay envelope without beating.

The main aim of this study was to explore whether some stringed instruments are more prone to the double-decay phenomenon than others. A simple criterion was advanced, equally appropriate to both physical mechanisms, which provides a necessary condition for a strong double decay. One of the modes of the vibrating string(s) must have damping due to energy loss into the instrument body, which is significantly bigger than the intrinsic damping in order to create a strong contrast of loss factors between the two relevant modes.

Plots have been presented, applying this criterion to the five instruments by making use of measured bridge admittances. Previous research (Woodhouse, 2017; Woodhouse *et al.*, 2021a) had already shown that in classical or X-braced guitars, loss into the body is usually surprisingly weak. The results presented in Fig. 3 confirm this conclusion: except near a few strong resonances at low frequency, such guitars are relatively unlikely to show significant double decays.

However, the other plots suggest that the guitar is somewhat of an exception among the instruments considered here. In keeping with the original conclusions of Weinreich (1977), Fig. 2(b) shows that the piano should indeed exhibit strong double-decay behaviour over a wide range of played notes. The lute and the mandolin both feature paired strings, and the results in Figs. 4 and 5 suggest that both instruments may show double decays over at least part of their range. The detailed patterns are different, though. In the particular mandolin measured, the effect is only predicted to appear above the lowest octave of playing range, whereas for the lute it is more widespread—but not as universal as in the piano.

Finally, the banjo shows a different trend from the other instruments. Despite having only single strings, it should show strong double-decay behaviour over most of its range, ever more so as frequency increases. Reassuringly, such envelope shapes have indeed been reported in previous literature (Stephey and Moore, 2008). The explanation lies in the higher bridge admittance arising from the use of a membrane rather than a wooden plate as the "soundboard."

ACKNOWLEDGMENTS

The author thanks Evan Davis for valuable discussions and feedback and two anonymous reviewers for helpful comments.

Carcagno, S., Bucknall, R., Woodhouse, J., Fritz, C., and Plack, C. J. (**2018**). "Effect of back wood choice on the perceived quality of steel-string acoustic guitars," J. Acoust. Soc. Am. **144**, 3533–3547.

Chaigne, A., and Kergomard, J. (**2013**). *Acoustics of Musical Instruments* (Springer Verlag, New York), p. 13.3.5.

Crandall, S. H. (**1970**). "The role of damping in vibration theory," J. Sound Vib. **11**(1), 3–18.

Cremer, L., Heckl, M., and Petersson, B. A. T. (**2005**). *Structure-Borne Sound*, 3rd ed. (Springer, New York).

Fletcher, N. H., and Rossing, T. D. (**1998**). *The Physics of Musical Instruments*, 2nd ed. (Springer, New York).

Lee, N., Smith, J. O., and Välimäki, V. (**2010**). "Analysis and synthesis of coupled vibrating strings using a hybrid modal-waveguide synthesis model," IEEE Trans. Audio Speech Lang. Process. **18**, 833–842.

Lyon, R. H., and DeJong, R. G. (**1995**). *Theory and Application of Statistical Energy Analysis*, 2nd ed. (Butterworth-Heinemann, Boston, MA).

Martin, D. W. (**1947**). "Decay rates of piano tones," J. Acoust. Soc. Am. **19**, 535–541.

Newland, D. E. (**1989**). *Mechanical Vibration Analysis and Computation* (Longman Scientific and Technical, Harlow, UK).

Perkins, N. C., and Mote, C. D. (**1986**). "Comments on curve veering in eigenvalue problems," J. Sound Vib. **106**(3), 451–463.

Rayleigh, J. W. S. (**1945**). *The Theory of Sound*, 2nd ed. (Dover Publications, New York).

Skudrzyk, E. (**1980**). "The mean-value method of predicting the dynamic-response of complex vibrators," J. Acoust. Soc. Am. **67**(4), 1105–1135.

Stephey, L. A., and Moore, T. R. (**2008**). "Experimental investigation of an American five-string banjo," J. Acoust. Soc. Am. **124**, 3276–3283.

Valette, C. (**1995**). "The mechanics of vibrating strings," in *Mechanics of Musical Instruments*, edited by A. Hirschberg, J. Kergomard, and G. Weinreich (Springer-Verlag, New York), Chap. 4, pp. 116–183.

Välimäki, V., Huopaniemi, J., Karjalainen, M., and Jànosy, Z. (**1996**). "Physical modeling of plucked string instruments with application to real-time sound synthesis," J. Audio Eng. Soc. **44**, 331–353.
Weinreich, G. (**1977**). "Coupled piano strings," J. Acoust. Soc. Am. **62**(6), 1474–1484.
Woodhouse, J. (**2004a**). "On the synthesis of guitar plucks," Acta Acust. united Ac. **90**(5), 928–944.
Woodhouse, J. (**2004b**). "Plucked guitar transients: Comparison of measurements and synthesis," Acta Acust. united Ac. **90**(5), 945–965.
Woodhouse, J. (**2017**). "Influence of damping and nonlinearity in plucked strings: Why do light-gauge strings sound brighter?," Acta Acust. united Ac. **103**(6), 1064–1079.
Woodhouse, J. (**2021**). "Euphonics: The science of musical instruments," https://euphonics.org/7-3-multiple-strings-and-double-decays/ (Last viewed October 27, 2021).
Woodhouse, J., and Lynch-Aird, N. J. (**2019**). "Choosing strings for plucked musical instruments," Acta Acust. united Ac. **105**, 516–529.
Woodhouse, J., Manuel, E. K. Y., Smith, L. A., Wheble, A. J. C., and Fritz, C. (**2012**). "Perceptual thresholds for acoustical guitar models," Acta Acust. united Ac. **98**(3), 475–486.
Woodhouse, J., Politzer, D., and Mansour, H. (**2021a**). "Acoustics of the banjo: Measurements and sound synthesis," Acta Acust. **5**, 15.
Woodhouse, J., Politzer, D., and Mansour, H. (**2021b**). "Acoustics of the banjo: Theoretical and numerical modelling," Acta Acust **5**, 16.